Dalton Transactions

Observation of Current Rectification by a New Asymmetric Iron(III) Surfactant in a Eutectic GaIn | LB Monolayer | Au Sandwich

Journal:	*Dalton Transactions*
Manuscript ID	DT-ART-02-2018-000562.R1
Article Type:	Paper
Date Submitted by the Author:	18-Mar-2018
Complete List of Authors:	Johnson, Marcus; University of Alabama, Chemistry and Biochemistry Horton, Chad; Alabama State University College of Health Sciences, Chemistry and Biochemistry Gonawala, Sunalee; Wayne State Univeristy, Chemistry Verani, Claudio; Wayne State University, Chemistry Metzger, Robert M.; University of Alabama, Chemistry

Journal Name

ARTICLE

Observation of Current Rectification by a New Asymmetric Iron(III) Surfactant in a Eutectic GaIn|LB Monolayer|Au Sandwich

Received 00th January 20xx,
Accepted 00th January 20xx

DOI: 10.1039/x0xx00000x

www.rsc.org/

Marcus S. Johnson,[a] Chad L. Horton,[a] Sunalee Gonawala,[b] Cláudio N. Verani,*[,b] and Robert M. Metzger*[,a]

In this paper we expand on the search for molecular rectifiers of electrical current and report on a hexacoordinate metallosurfactant [Fe^{III} (L^{N3O})$(OMe)_2$], where $(L^{N3O})^-$ is the deprotonated form of the new asymmetric ligand 2-((E)-((4,5-bis (2-methoxyethoxy)-2-(((E)–pyridin-2-ylmethylene)amino)phenyl)imino)methyl)-4,6-di-tert-butyl-phenol. This species rectifies current when deposited as Langmuir-Blodget film in a "EGaIn/Ga_2O_3 | LB | Au" sandwich with rectification ratios ranging from 25 to 300 at 1 Volt.

Introduction

Over 40 years ago Aviram and Ratner[1] proposed that a single molecule consisting of an electron donor region (D) and a separate electron acceptor region (A) could be a rectifier of electrical current, in analogy to inorganic bulk pn junction rectifiers. This idea, verified many times for over 50 molecules[2] implies that a directional electron transfer can also occur via the frontier orbitals of a single molecule.

The use of transition metal complexes in "electrode|molecule" junctions has developed rather slowly, likely due to a reliance on symmetrical complexes such as nickel and copper phthalocyanines.[3]-[6] An early example of rectification mediated by d-orbitals in an asymmetric system was attained when a Ru(II) ion was coordinated to a thiophene-functionalized bipyridine ligand, and improved conjugation was attributed to the planarity acquired upon metallation.[7]

More recently the Verani group has determined that the high-spin five-coordinate $3d^5$ [Fe^{III}(L^{N2O3})] metallosurfactant[8] with a tris-phenolate ligand‡ **(Figure 1**, structure **2)** displays current rectification when a Langmuir-Blodgett (LB) monolayer is placed between Au electrodes represented here as "Au|LB|Au".[,10] Top Au electrode areas of about 0.3 × 0.8 mm^2 = 0.24 mm^2 were reported with 1.5 nA of enhanced current. A similar species [Fe^{III}(L^{N2O2})Cl] **(Figure 1**, structure **1)** with a related bis-phenolate ligand§ and a monodentate chloride ligand (Cl) occupying the axial position[9] conserves the rectifying behavior, albeit with the onset of rectification starting at a lower threshold. The rectification ratios $RR(V) \equiv -I(V)/I(-V)$ for **1** ranged between 3.99 and 28.6 at V = 2 V, and between 2.04 and 31 at V = 4 V. As measurements were repeated, the *RR* values became smaller, and the *IV* response tended to become more symmetric. The beginning of rectification (deviation from ohmic, or linear, IV behavior) appeared at about 0.6 V, and the currents were fairly low. The rectification of **1** using eutectic gallium/indium and gold electrodes was reported recently, with *RR* between 3 and 12 at ±0.7 V, and *RR* between 50 and 140 at ±1 V.[10] This assembly is represented as "Ga_2O_3/EGaIn|LB" monolayer of **1**|Au. Here Ga_2O_3/EGaIn is a eutectic GaIn droplet covered by a very thin and disordered adventitious Ga_2O_3 oxide formed by contact with air.[11] For this droplet the term EGaIn has been popularized.[12],[13] These three species are shown in **Figure 1** using a ionic model with attributed localized charges.

In this paper we investigate a new rectifying metallosurfactant, namely [Fe^{III} (L^{N3O})$(OMe)_2$] **(3)**. This species is based on a new asymmetric HL^{N3O} ligand containing a pyridine and phenolate moieties tethered by a phenylenediamine bridge, and is expected to intensify orbital distortions that lead to current rectification.

Results and discussion

Rationale for ligand design: We have recently proposed that distorted singly-occupied molecular orbitals (SOMO) with metallic character facilitate electron transfer in asymmetric current rectification. Having established that phenolate-rich asymmetric Fe^{III} complexes are capable of current rectification in Au|molecule|Au sandwiches, we hypothesize that the incorporation of electron deficient pyridine groups to the ligand framework will lower the SOMO energy levels and enable directional electron transfer.

[a] *Laboratory for Molecular Electronics, Department of Chemistry and Biochemistry, University of Alabama, Box 870336, Tuscaloosa, AL 35487, USA.*
Department of Chemistry, Wayne State University, 5101 Cass Avenue, Detroit, MI 482302, USA
Electronic Supplementary Information (ESI): Numerical data and plots of Figures 3 to 6 including the sweep identifiers

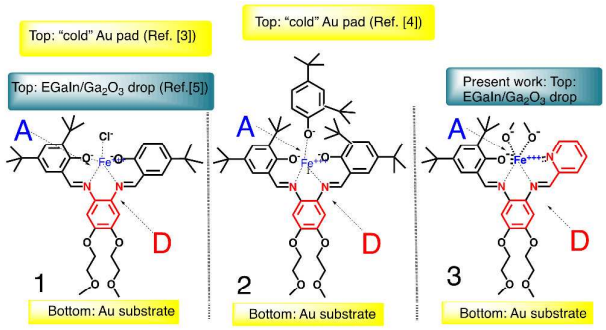

Figure 1. Three Fe^{III} metallosurfactants are monolayer rectifiers: **1**, **2**, and **3**. The red and blue zones indicate electron donor and acceptor regions.

Syntheses and characterizations: The ligand **[H_2L^{N3O}]** was synthesized by reacting one equivalent of 4,5-bis(2-methoxyethoxy)benzene-1,2-diamine with one equivalent of pycolinaldehyde under an inert atmosphere, followed by insertion of 3,5-di-*tert*-butyl-2-hydroxybenzaldehyde. The synthetic schemes are shown in **Scheme 1**. The recrystallized ligand was treated with excess anhydrous sodium methoxide and then with one equiv. of iron(III) chloride under reflux to yield a microcrystalline powder. In spite of multiple attempts we were not able to obtain X-ray quality crystals.

The IR spectroscopic data for **3** showed symmetric and asymmetric C–H stretching vibrations in the regions of ~ 2810-2970 cm^{-1} and a prominent peak at 1582 cm^{-1} belonging to the C=N stretching vibrations. The high resolution ESI-MS data showed $[M - (OCH_3)^-]^+$ at m/z = 647.2651 in excellent agreement with a calculated value of 647.2658. Isotopic patterns are in good agreement with experimental and simulated data.

The UV-visible spectrum of **3** was recorded in a 1.0×10^{-5} mol L^{-1} CH_2Cl_2 solution and showed intense absorption bands in the 300-700 nm region. A predominant band at 340 nm region shows ε ≈ 24,000 L mol^{-1} cm^{-1} along with several shoulders at 310, 320 and 352 nm. This band is attributed to ligand-to-metal charge transfer originating from phenylenediamine- and/or phenolate-based p_π-orbitals to d_{σ^*} and d_{π^*} Fe^{III}-based orbitals.[14], [15] Interestingly, the intensity of these bands in **3** is approximately half of that observed for the related system **1** with two phenolates.[9] Bands between 400-700 nm consisted of intra-ligand π→π* charge transfer, as observed for similar species [16] and by calculations. Complex **3** shows evidence of strong covalent bonds, as observed by the presence of ligand-to-metal charge transfer processes.

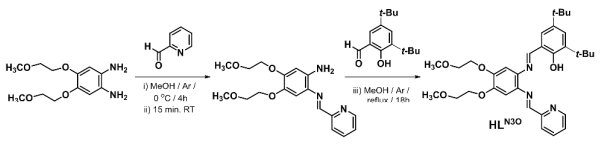

Scheme 1. Synthetic route of ligand HL^{N3O}

The complex showed a quasi-reversible single-electron reduction process at -0.48 $V_{Fc/Fc+}$ (ΔE_p= 0.08 V, $|I_{pa}/I_{pc}|$ = 1.5) in CH_2Cl_2, tentatively assigned to the Fe^{III}/Fe^{II} reduction couple. In our systems the Fe^{III}/Fe^{II} redox couples for $[N_2O_3]$ environments with electron donating *t-butyl* phenolate moieties are observed[8],[14] around -1.5 $V_{Fc/Fc+}$, whereas **3** with a $[N_3O]$ donor set shows a less negative potential. This is attributed to the lower electron density around the metal center associated with the removal of one phenolate. Processes tentatively attributed to the ligand[14],[15],[17],[18] are observed at 0.48 $V_{Fc/Fc+}$ (ΔE_p= 0.06 V, $|I_{pa}/I_{pc}|$ = 13.8) and E_{pa} = 0.79 V, and assigned to the phenelenediamine and phenolate oxidations, respectively.

Based on these properties we describe **3** as having the $[N_3O]$ donors of the deprotonated ligand equatorially bound to those Fe^{III} orbitals with components along the x and y axes, whereas two monodentate methoxy groups[19],[20],[21] complete a pseudo-octahedral geometry along the z axis. The metallosurfactant has hydrophilic portions at the distal alkoxo chains, and a hydrophobic region, thanks to the *tert*-butyl groups. The region around the Fe^{III} ion is also hydrophilic but the axial methoxy ligands shelter this hydrophilic region.

Pockels-Langmuir monolayer of 3: The measurement protocol used here replicates the protocol published elsewhere,[11] A solution of **3** in $CDCl_3$ (1 mg/mL) was placed in a NIMA (Coventry, UK, now Biolin, Espoo, Finland) film balance. The surface pressure-area (Π-A) isotherm was measured at room temperature (**Figure 2**).

The Pockels-Langmuir film (*i.e.* the monolayer at the air-water interface) was compressed and expanded at relatively low coverage (large area) to probe the reversibility of the isotherm, and, instead of heading to film collapse, the film pressure was monitored as the solution was slowly added, until small 3-dimensional gold-colored crystals were observed:

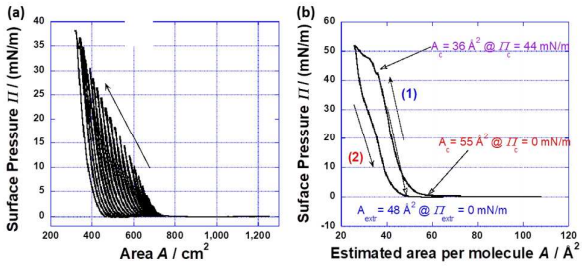

Figure 2. Surface pressure *vs.* area isotherms for **3:** (a) showing successive cycles of compression and subsequent expansion; (b) showing distinct paths for compression (path 1) and expansion (path 2).

this is the equilibrium spreading pressure (ESP):[22] Π_{ESP} = 13.5 to 14 mN/m; the area at this pressure A_{ESP} was about 100 $Å^2$. The isotherm was studied by gradually increasing the maximum film pressure (**Figure 2a**): the isotherm shifted toward smaller areas, either because some molecules at the air-water interface were incrementally pushed into the aqueous subphase, or because the molecules would start to ride over each other. There is some minor hysteresis in each

cycle. The arrow indicates that as the pressure limit is increased and the isotherm is cycled anew, the area of the monolayer shrinks linearly with time, suggesting that either the molecules are gradually dissolved into the aqueous subphase, or the molecules tumble atop each other.[23] Thus the horizontal axis cannot be converted into area per molecule, since the number of molecules in the monolayer is uncertain. These results indicate that the metallosurfactant **3** deviates from the ideal Ries mechanism expected for monolayers of organic surfactants, which includes well-defined folding, bending, and breaking into multilayers at collapse.[24] The non-amphiphilic C_{60} also exhibited extreme aggregation: this was prevented by using a very dilute dropping solution.[25]

The surface pressure Π vs. area A isotherm of **3** shows path (1) upon film compression and a different path (2) upon subsequent expansion: there is some hysteresis. The horizontal axis, in Å^2 per molecule, is calculated from the leftmost isotherm of **Figure 2A**, assuming zero mass loss at the interface. Three values for the surface pressure and area per molecule obtained from **Figure 2b** are: at film collapse Π_c = 44 mN/m and A_c = 36 Å^2 molecule^{-1}; at initial pressure Π_o = 0 mN/m and A_o = 55 Å^2 molecule^{-1}; at extrapolated pressure Π_{extr} = 0 mN/m and A_{extr} = 48 Å^2 molecule^{-1}.

Langmuir-Blodgett monolayer films: PL monolayers of **3** were transferred on the upstroke (15 mm / min) onto Si at the ESP (with transfer ratio 1.0), and also onto Si wafers covered with a fresh thermally evaporated hydrophilic Au film (Au thickness 150 nm atop an adhesion layer of ca. 30 nm of W), forming in each case a Z-type LB monolayer on the substrate.

"EGaIn/Ga_2O_3|LB3|Au" sandwiches: Although cleaner results could be expected with a top cold gold electrode,[8] we opted to use the GaIn eutectic (EGaIn) liquid-drop top electrode instead, so as to compare the present results for **3** with the recently studied species **1**.[10] Here we use the term "sandwich"[2] to describe the device made with a top EGaIn drop on an LB monolayer atop a bottom Au electrode. For these metal-molecule-metal assemblies, most people use the term "junction", but "junction" is also used for a single interface as in *e.g.* metal to semiconductor, or metal to organic molecule. Using "sandwich" makes it clear that we have two interfaces on the both sides of a molecule or monolayer.

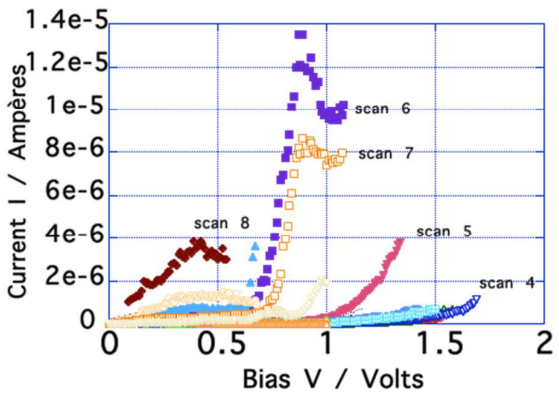

Figure 3. Initial evaluation of the "EGaIn/Ga_2O_3 | LB**3** | Au" sandwich.

Direct-current (DC) *IV* electrical measurements were made on the "EGaIn/Ga_2O_3|LB of **3**|Au" sandwiches using a Keithley 236A Source-Measure Unit connected to a PC under program control. The bottom Au electrode was linked by a clamp to one measuring electrode. As previously,[10] the top electrode was

Table 1. Initial evaluation of 23 scans of "EGaIn/Ga_2O_3| LB**3**|Au" sandwiches. V_{max} is the maximum bias (Volts) before sandwich failure and I_{max} is the current (μA) at V_{max}.

Scan	V_{max}	I_{max}	Scan	V_{max}	I_{max}
01	1.33	0.367	**13**	1.00	0.045
02	1.52	0.309	**14**	1.50	0.709
03	1.58	0.666	**15**	1.07	7.98
04	1.69	1.11	**16**	1.00	0.177
05	1.34	3.81	**17**	1.07	7.98
06	1.08	10.2	**18**	1.00	0.177
07	1.16	0.708	**19**	1.00	0.018
08	0.54	3.00	**20**	1.00	1.8
09	1.43	0.694	**21**	1.00	0.112
10	0.67	3.64	**22**	0.87	31.9
11	1.00	0.015	**23**	1.00	0.000

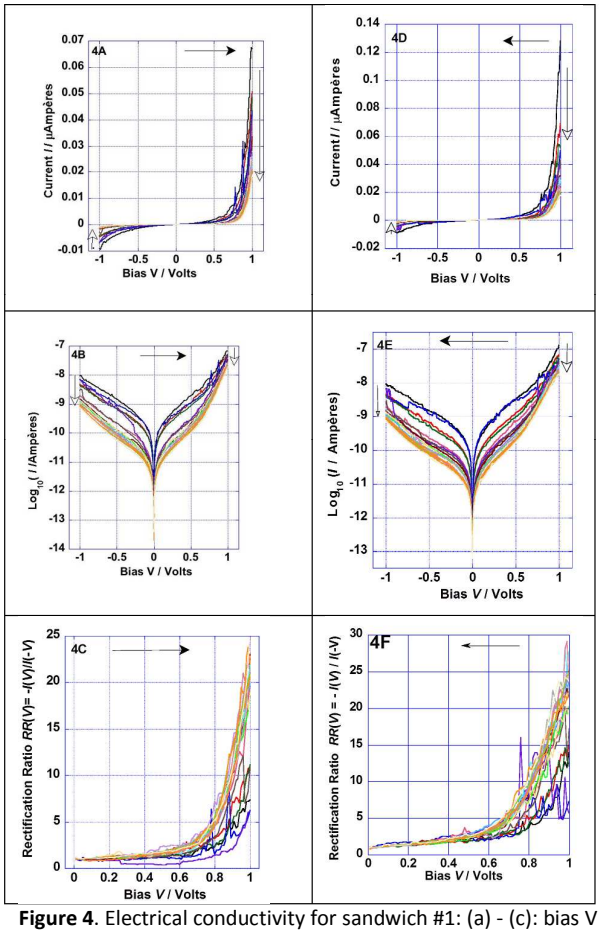

Figure 4. Electrical conductivity for sandwich #1: (a) - (c): bias V increasing (→) (d) - (f): V decreasing (←); (a) & (d): *I* vs. *V*; (b) & (e) log| *I* | vs. *V*; (c) & (f): rectification ratios $RR(V) \equiv I(V)/I(-V)$. Vertical open arrows show trend as scans are repeated.

atop the LB monolayer formed by gradually moving a conical EGaIn drop (1 mm diameter, 2 mm long, delivered by a plastic syringe and connected to a hook in a Au wire). The current *I* was monitored at a low bias (*V* = 0.0001 V) as the droplet was lowered very gently using a mechanical micromanipulator (Parker Daedal Division) in an open custom-built steel Faraday cage[26] mounted on a polyurethane base to reduce ambient vibrations until electrical contact was made. An initial contact current (ICC) of 1 nA or less chronicled a successfully formed sandwich. Sandwiches without such ICC were not studied further. After this initial electrical contact was made, the Faraday cage was closed.

The *IV* measurements on the "EGaIn/Ga_2O_3|LB of **3**|Au" sandwiches proceeded in two phases. In the initial, exploratory phase, sandwiches were studied to find the bias tolerated before either open circuits or short circuits set in (**Figure 3)**. **Table 1** and **Figure 3** display the initial evaluation of 23 scans of "EGaIn/Ga_2O_3|LB**3**|Au" sandwiches. This initial evaluation reveals the following: (i) the currents across the monolayer of **3** are smaller than those seen for **1**, (ii) 19 of 23 scans are stable to 1 V; (iii) scans 5, 6, 15, and 22 have much larger currents at 1 V than the others (iv) 6 scans out of 23 are stable well past 1 V. We therefore decided to study the rectification properties of the sandwich "EGaIn/Ga_2O_3|LB of **3**|Au" within the bias range of ±1 V.

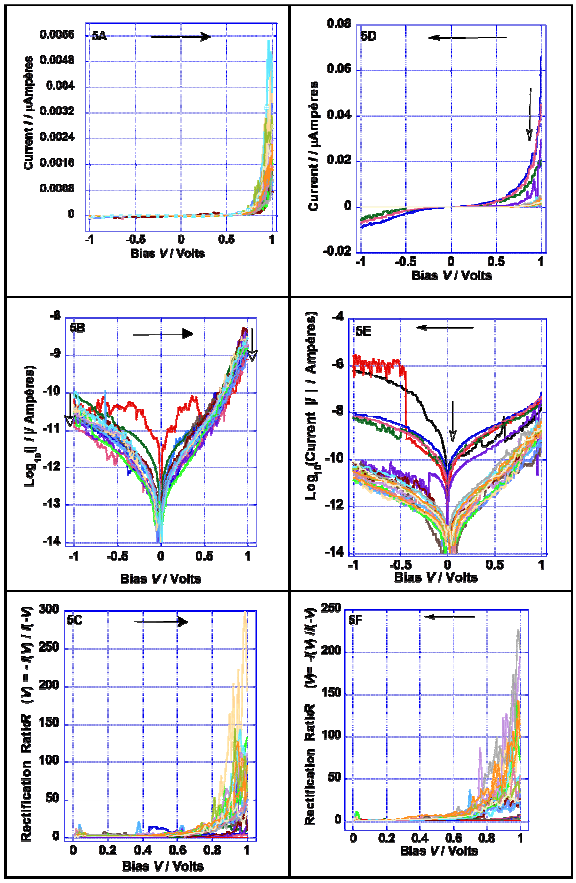

Figure 5. Electrical conductivity for sandwich #2: (a) - (c): bias *V* increasing; (d) - (f) *V* decreasing (indicated by top arrows). (a) and (d): *I* vs. *V*; (b) and (e): $\log_{10}|\ I\ |$ vs. *V*; (c) and (f): rectification ratios $RR(V) \equiv I(V)/I(-V)$.

The second phase studied a sandwich repetitively (multiple "sweeps") until a short circuit developed. Three sandwiches were studied successfully between -1 and 1 V. The data for sandwiches #1, #2, and #3 are shown in **Figures 4**, **5**, and **6**, respectively. As usual, the sandwiches were swept boustrophedonically (i.e. in opposite directions in successive rows; the bias was increased in one sweep, then decreased on the next sweep, etc). The data for increasing V differ slightly from the data for decreasing V.

The results offer compelling evidence to support species **3** as being a molecular rectifier of electrical current, in analogy to the previously studied compounds **1** and **2**.[8]-[10] However, some aspects require further discussion, as the three sandwiches for **3** exhibit different currents at 1 V. On one hand, sandwich #1 shows current up to 0.07 μA and 0.14 μA (**Figures 4A** and **4D**, respectively), while sandwich #3 reaches 0.03 and 0.09 μA (see **Figures 6A and 6D**). On the other hand, sandwich #2 shows considerable smaller currents up to 0.0056 and 0.078 μA (**Figures 5A and 5D**, respectively).

These pad-to-pad variations in total current at 1 V (lowest factor of 0.14 μA / 0.0056 μA = 25) are an unfortunate consequence of the measuring technique.[26] This variability was also encountered and discussed critically in sandwiches composed of "EGaIn|Ga_2O_3|cold-Au|n-alkanethiols|Au^{TS}",[28] where Au^{TS} indicates template-stripped Au.[29] These currents are also lower than seen for compound **1**, as noted earlier;[10] the maximum rectification ratios for sandwich #1 reach *RR* =

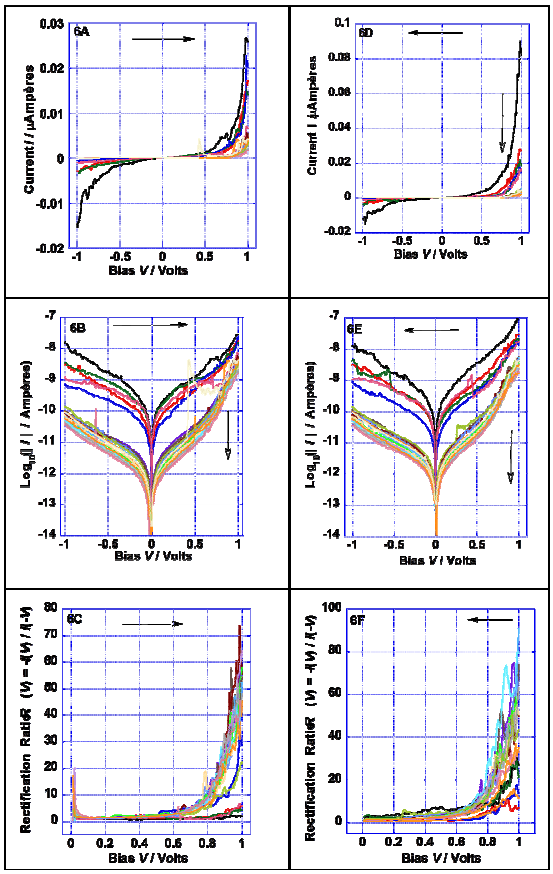

Figure 6. Electrical conductivity for sandwich #3: (a)-(c): bias *V* increasing (→); (d)-(f): *V* decreasing (←); (a) and (d): *I* vs. *V*; (b) and (e): $\log_{10}|\ I\ |$ vs. *V*; (c) and (f): rectification ratios $RR(V) \equiv I(V)/I(-V)$.

25 to 30 (**Figures 4C** and **4F**, respectively); they are *RR* = 300 to 250 for sandwich #2 (see **Figures 5C** and **5F**), which had such low currents; they are *RR* = 80 to 90 (see **Figures 6C** and **6F)** for sandwich #3. Numerical data and sweep history are detailed in the ***Electronic Supplementary Information***.

Mechanistic inferences: The currently used rectification model assumes that the metal electrode Fermi level (E_F) is approximately 1 eV lower than the energy of the lowest half-occupied SOMO of the molecular species to enable electron transfer.[8]-[10],[30] On one hand, values of E_F energies for EGaIn[12] and gold[31],[32],[33] electrodes have been reported respectively at -4.2 and -5.1 eV below vacuum. On the other hand redox potentials of metallosurfactant **3** measured via cyclic voltammetric methods can be converted to comparable solid-state potentials following well-established procedures [34],[35],[36],[37] to obtain a value of -4.7 eV for the SOMO in **3.** Considering the asymmetry of the molecule, this MO is likely a linear combination of t_{2g}-like orbitals. Therefore, **Figure 7** shows that the EGaIn Fermi levels are approximately 0.5 eV above the Fe-based SOMO, whereas the Au Fermi levels are 0.4 V below. Electron transfer is certain to occur when an appropriate bias is applied, the SOMO gets populated thus forming an Fe^{II} state. Alternatively, electrons from the EGaIn electrode may occupy other higher energy e_g-like SOMOs forming an excited $(Fe^{II})^*$ state. The excited electron can transfered to the Au electrode either directly or via d-d d decay that lowers the energy of the resulting doubly occupied MO prior to transfer. The ligand-based and doubly occupied HOMO is found at 1.3 eV below the Au electrode, and does not contribute in electron transfer.

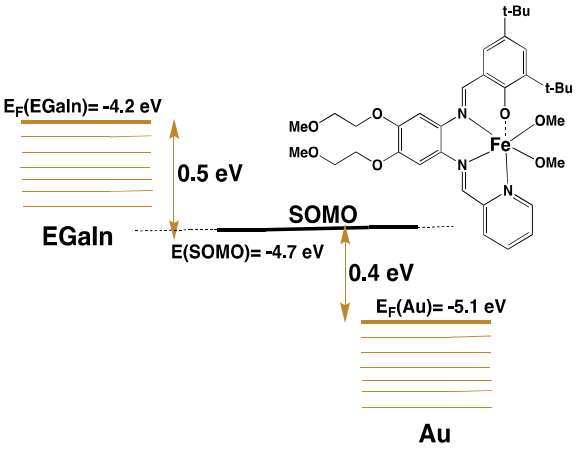

Figure 7. Energetics of Fermi levels in EGaIn and Au electrodes as compared to the molecular metallosurfactants **3.**

Conclusions

The metallosurfactant **$[Fe^{III}(L^{N3O2})]$ (3),** placed as a Langmuir Blodgett monolayer film between a Au electrode and a soft contact of gallium indium eutectic (EGaIn), is a rectifier (maximum *RR* = 300 at ± 1 V) in analogy with previously studied metallosurfactants **1** and **2**. This is the first example of Fermi/SOMO analysis of electron transfer involving a molecular metallosurfactants and EGaIn/Au sandwiches. Future studies will delve deeper into the proposed mechanisms relying on new asymmetric Fe-containing surfactants and on DFT orbital analysis to complement the experimental evidence.

Experimental

General. Reagents and solvents were used as received from commercial sources. Infrared spectra were recorded from 4000-650 cm^{-1} as KBr pellets on a Bruker Tensor 27 FTIR spectrophotometer. ^{1}H-NMR spectra for the ligand were obtained in a Mercury FT-NMR 400 MHz or a Varian VNMRS 500 MHz instrument using $CDCl_3$ as solvent. ESI-(+) mass spectrometry was performed in a triple quadrupole Micromass Quarttro LC equipment. Elemental analysis for C, H and N was carried out using an Exeter CHN analyzer by Midwest Microlab in Indianapolis, Indiana, USA. UV-Visible spectra were obtained with quartz cells at room temperature in a UV-3600 Shimadzu spectrophotometer operating in the range of 190 to 1600 nm. Cyclic voltammograms were collected on a BAS 50W potentiostat/galvanostat at room temperature in 1.0 × 10^{-3} mol L^{-1} CH_2Cl_2 solutions containing 0.1 M of *n*-Bu_4NPF_6 as the supporting electrolyte under an inert atmosphere. The electrochemical cell was comprised of Glassy carbon (working), Ag/AgCl (reference), Pt wire (auxiliary electrode). The ferrocene/ferrocenium redox couple Fc/Fc^+ ($E° = 400$ mV *vs*. NHE) was used as the internal standard.[38] Pockels-Langmuir and Langmuir Blodgett films were deposited using a a NIMA (Coventry, UK; now Biolin, Espoo, Finland) balance. Pressure-area isotherms were measured at room temperature.

Synthesis of the ligand HL^{N3O}. To a stirred mixture of 4,5-bis(2-methoxyethoxy) benzene-1,2-diamine in dry MeOH, one equiv. of pyridine-carboxaldehyde dissolved in dry MeOH was added dropwise over 30 min. at 0 °C. The solution was stirred for 4 h at 0 °C and then for 15 min. at room temperature. Then 1 equiv. of 3,5-di-tert-butyl-2-hydroxy benzaldehyde dissolved in dry MeOH was added dropwise and kept under mild reflux for 18 h. The whole procedure was performed under inert atmosphere. The solvent was removed by rotary evaporation and the resulting brown oily product was purified using column chromatography with silica as stationary phase and hexane:ethyl acetate (1:1) as eluent. Yield: 38 %. ESI (m/z^+) in CH_2Cl_2 = 562.31 for $[C_{33}H_{43}N_3O_5+H^+]$; ^{1}H NMR, ppm ($CDCl_3$, 400 MHz): 1.06-1.48 (m, $18H^{tBu}$), 3.47 (s, $6H^{OCH3}$), 3.77-3.82 (m, $4H^{OCH2}$), 4.14-4.31 (m, $4H^{OCH2}$), 6.96 (s, $1H^{ph}$), 7.09 (s, $1H^{ph}$), 7.28 (d, $1H^{ph}$), 7.49(m, $2H^{py}$), 7.89 (td, $1H^{py}$), 8.26 (d, $1H^{ph}$), 8.47 (s, $1H^{CH}$), 8.62 (dd, $1H^{py}$), 8.66 (s, $1H^{CH}$). IR (KBr, cm^{-1}): 3245 (ν_{O-H}), 2871-2954 (ν_{C-H}), 1642 ($\nu_{C=C}$, aromatic), 1509 ($\nu_{C=C}$, aromatic), 1600 ($\nu_{C=N}$), 1258 (ν_{C-O-C}), 1124 (ν_{C-O-C}).

Synthesis of $[Fe^{III}(L^{N3O2})Cl]$ (3): A solution of H_2L^{N3O2} (0.25 g, 0.36 mmol) containing anhydrous sodium methoxide (0.04 g, 0.73 mmol) in a 1:1 MeOH:CH3Cl mixture was treated with $FeCl_3.6H_2O$ (0.10 g, 0.36 mmol). The resulting solution was kept under mild reflux for 4 h, and then cooled to room

temperature. The crude product was filtered off and recrystallized at ambient conditions to yield greenish brown microcrystals. Yield: 78 %. ESI (m/z^+) in methanol = 647.2651 (100%,) for $[M - (OCH_3)^-]^+$, with m/z^+ calculated at 647.2658) Anal. Calc. for $[C_{35}H_{48}FeN_3O_7]$: C, 61.95; H, 7.13; N, 6.19%. Found: C, 61.57; H, 6.85; N, 5.97%. IR (KBr, cm-1) 2872-2957 (νC-H), 1638 (νC=C, aromatic), 1582 (νC=N), 1502 (νC=C, aromatic), 1255 (νC-O-C), and 1126 (νC-O-C).

Fabrication of EGaIn/Ga_2O_3|LB3|Au sandwiches: As in previous work,[10],[11] the bottom Au electrode (ca. 150 nm thick) was fabricated by direct evaporation of Au pellets onto a Si substrate pre-coated by a 30 nm thick W adhesion layer in an Edwards 308 evaporator; as soon as taken out of the vacuum chamber, this Au-bearing substrate was rapidly put under conductivity H_2O (Barnstead ion-exchange resin, 18.2 MΩ resistivity) in a NIMA film balance (to preserve its hydrophilic surface). A monolayer of **3** was transferred on the upstroke onto this hydrophilic Au surface. The remaining procedure has been described above.

The variation in the electrical currents reported here between the three sandwiches, and particularly between successive sweeps may have multiple causes:[2] metal electromigration under bias, surface oxidation of Ga, thermal re-ordering. The best present recourse is in many repeated measurements.

Conflicts of interest

There are no conflicts of interest to declare.

Acknowledgements

The authors thankfully acknowledge support from the National Science Foundation through grants NSF-CHE-0848206 (RMM) and NSF-CHE-1012413 and NSF-CHE-1500201 (CNV). This includes financial support for M.S.J. and S.G.

Notes and references

‡ The ligand $(L^{N2O3})^{-3}$ is the deprotonated form of H_3L^{N2O3}, or (E)-6,6'-(((2-((3,5-di-tert-butyl-2-hydroxybenzylidene)amino)-4,5-bis(2-methoxyethoxy)phenyl)azanediyl)bis(methylene)) bis(2,4-di-tert-butylphenol)

§ The ligand $(L^{N2O2})^{-2}$ is the deprotonated form of 6,6'-(1*E*,1'*E*)-(4,5-*bis*(2-methoxyethoxy)-1,2phenylene)*bis*(azanylylidene) *bis*(methanylylidene)*bis*(2,4-di-tert-butylphenol).

1 A. Aviram, M. A. Ratner, *Chem. Phys. Lett.* 1974, **29**, 277-283.
2 R. M. Metzger, *Chem. Rev*. 2015, **115**, 5056-5115.
3 G. J. Ashwell, B. Urasinska, W. D. Tyrrell, *Phys. Chem. Chem. Phys*. 2006, **08**, 3314-3319.
4 W. J. Pietro, *Adv. Mater.* 1994, **06**, 239-242.
5 S. Roth, S. Blumentritt, M. Burghard, C. M. Fischer, G. Philipp, C.-M. Schwanneke, *Synth. Metals* 1997, **86**, 2415-2418.
6 M. H. Yoon, A. Facchetti, T. J. Marks, *Proc. Natl. Acad. Sci. U.S.* 2005, **102**, 4678-4682.
7 Y. Lee, S. Yuan, A. Sanchez, L. Yu, *Chem. Commun*. 2008, **02**, 247-249.
8 L. D. Wickramasinghe, M. M. Perera, L. Li, G. Mao, Z. Zhou, C. N. Verani, *Angew. Chem. Int. Ed.* 2013, **52**, 13346-13350.
9 L. D. Wickramasinghe, S. Mazumder, S. Gonawala, M. M. Perera, H. Baydoun, B. Thapa, L. Li, G. Mao, Z. Zhou, H. B. Schlegel, C. N. Verani, *Angew. Chem. Int. Ed.* 2014, **53**, 14462-14467.
10 M. S. Johnson, L. D. Wickramasinghe, C. N. Verani, R. M. Metzger, *J. Phys. Chem. C* 2016, **120**, 10578-10583.
11 M. S. Johnson, R. Kota, D. L. Mattern, C. M. Hill, M. Vasiliu, D. A. Dixon, R. M. Metzger, *J. Mater. Chem.* ***C*** 2014, 9892-9902.
12 R. C. Chiechi, E. A. Weiss, M. D. Dickey, G. W. Whitesides, *Angew. Chem. Int. Ed.* 2008, **47**, 142-144.
13 W. F. Reus, M. M. Thuo, N. D. Shapiro, C. A. Nijhuis, G. M. Whitesides, *ACS Nano* 2012, **06**, 4806-4822.
14 M. Allard, J. Sonk, M. J. Heeg, B. McGarvey, H. B. Schlegel, C. N. Verani *Angew. Chem. Int. Ed.* 2012**, 51**, 3178–3182
15 M. Lanznaster, H. P. Hratchian, M. J. Heeg, L. Hryhorczuk, B. R. McGarvey, H. B. Schlegel, C. N. Verani *Inorg. Chem.* 2006, **45**, 955-957.
16 O. Rotthaus, O. Jarjayes, C. Philouze, C. P. D. Valle, F. Thomas, *Dalton Trans.* 2009, **10**, 1792-1800.
17 A. Kochem, O. Jarjayes, B. Baptiste, C. Philouze, H. Vezin, K. Tsukidate, F. Tani, M. Orio, Y. Shimazaki, F. Thomas *Chem. Eur. J.* 2012, **18**, 1068.
18 R. C. Pratt, T. D. Stack, *J. Am. Chem. Soc.* 2003, **125**, 8716.
19 R. Shakya, M. Allard, M. J. Heeg, J. Shearer, B. McGarvey, C. N. Verani *Inorg. Chem.* 2011, **50**, 8356–8366.
20 G. Wu, F. Mei, Q. Gao, F. Han, S. Lan, J. Zhang and D. Li *Dalton Trans.*, 2011, **40**, 6433-6439.
21 F. Mei, C. Ou, G. Wu, L. Cao, F. Han, X. Meng, J. Li, D. Li and Z. Liao *Dalton Trans.*, 2010, **39**, 4267–4269.
22 A. W. Snow, G. G. Jernigan, M. G. Ancona, *Thin Solid Films* 2014, **556**, 475-484.
23 R. Shakya, S. S. Hindo, L. Wu, M. Allard, M. J. Heeg, H. P. Hratchian, B. R. McGarvey, S. R. P. da Rocha, C. N. Verani *Inorg. Chem.* 2007, **46**, 9808-9818.
24 H. E. Ries, Jr. *Nature* 1979, **281**, 287–289.
25 P. Wang, Y. Maruyama, and R. M. Metzger *Langmuir* 1996, **12**, 3932-3937.
26 R. M. Metzger, T. Xu, I. R. Peterson, *J. Phys. Chem. B,* 2001, **105**, 7280-7290.
27 W. F. Reus, C. A. Nijhuis, J. R. Barber, M. M. Thuo, S. Tricard, G. M. Whitesides, *J. Phys. Chem. C*, 2012, **116**, 6714-6733.
28 M. S. Johnson, C. L. Horton, M. R. A. Monnette, R. M. Metzger, *unpublished.*
29 P. Wagner, M. Hegner, H.-J. Güntherodt, G. Semenza, *Langmuir* 1995, **11**, 3867-3875.
30 L. D. Wickramasinghe, S. Mazumder, K. K. Kpogo, R. J. Staples, H. B. Schlegel, C. N. Verani, *Chem. Eur. J.* 2016*,* **22**, 10786-10790
31 L. Zhang, J. A. Bain, J. G. Zhu, L. Abelmann, T. Onoue, *IEEE Trans. Magn.* 2004, **40**, 2549-2551.
32 K. Kitagawa, T. Morita, S. Kimura, *Langmuir* 2005, **21**, 10624-10631.
33 K. Seo, A. V. Konchenko, J. Lee, G. S. Bang, H. Lee, *J. Am. Chem. Soc*. 2008, **130**, 2553-2559.
34 J. He, Q. Fu, S. Lindsay, J. W. Ciszek, J. M. Tour *J. Am. Chem. Soc.* 2006, **128**, 14828-14835.
35 K. W. Hipps, *Scanning Tunneling Spectroscopy. In Handbook of Applied Solid State Spectroscopy*, Vij, D. R., Ed., Springer-Verlag: Berlin, **2006**; Chapter 7.
36 L. Scudiero, D. E. Barlow, K. W. Hipps *J. Phys. Chem.B* 2002, **106**, 996-1003.
37 A. Schmidt, N. R. Armstrong, C. Goeltner, K. Muellen *J. Phys. Chem.* 1994, **98**, 11780-11785.
38 R. R. Gagne, C. A. Koval and G. C. Lisensky *Inorg. Chem.*, 1980, **19**, 2854-2855.